

## Video Article

# Construction and Operation of a Light-driven Gold Nanorod Rotary Motor System

Daniel Andrén<sup>1</sup>, Pawel Karpinski<sup>1</sup>, Mikael Käll<sup>1</sup><sup>1</sup>Department of Physics, Chalmers University of TechnologyCorrespondence to: Daniel Andrén at [daniel.andren@chalmers.se](mailto:daniel.andren@chalmers.se)URL: <https://www.jove.com/video/57947>DOI: [doi:10.3791/57947](https://doi.org/10.3791/57947)

Keywords: Engineering, Issue 136, Optical rotation, nanomotors, plasmonics, optical tweezers, Brownian motion, photothermal effects, LSPR spectroscopy

Date Published: 6/30/2018

Citation: Andrén, D., Karpinski, P., Käll, M. Construction and Operation of a Light-driven Gold Nanorod Rotary Motor System. *J. Vis. Exp.* (136), e57947, doi:10.3791/57947 (2018).

## Abstract

The possibility to generate and measure rotation and torque at the nanoscale is of fundamental interest to the study and application of biological and artificial nanomotors and may provide new routes towards single cell analysis, studies of non-equilibrium thermodynamics, and mechanical actuation of nanoscale systems. A facile way to drive rotation is to use focused circularly polarized laser light in optical tweezers. Using this approach, metallic nanoparticles can be operated as highly efficient scattering-driven rotary motors spinning at unprecedented rotation frequencies in water.

In this protocol, we outline the construction and operation of circularly-polarized optical tweezers for nanoparticle rotation and describe the instrumentation needed for recording the Brownian dynamics and Rayleigh scattering of the trapped particle. The rotational motion and the scattering spectra provides independent information on the properties of the nanoparticle and its immediate environment. The experimental platform has proven useful as a nanoscopic gauge of viscosity and local temperature, for tracking morphological changes of nanorods and molecular coatings, and as a transducer and probe of photothermal and thermodynamic processes.

## Video Link

The video component of this article can be found at <https://www.jove.com/video/57947/>

## Introduction

The methods presented in this article replicates those used in our previous work<sup>1</sup> to study nanoscale photothermal effects influencing light-driven gold nanorod rotary motors. Variants of the experimental platform has been used in several related publications<sup>2,3,4,5,6,7,8,9</sup>.

Optical tweezers are widely used for controlling position, force and linear momentum transfer at small length scales in physics, biology, and engineering<sup>10,11,12,13,14</sup>. Angular momentum carried by circularly polarized light can be employed for additional motion control because it continuously transfer torque to trapped objects<sup>15</sup>. By combining optical linear and angular momentum transfer, it is then possible to construct non-invasive rotary nanomotors with potential for diverse applications, such as drug delivery into single cells<sup>16,17</sup>, nanoscale surgery<sup>18</sup>, and active nanofluidics<sup>19</sup>, amongst others.

By using metallic nanoparticles as the subject of light driven manipulation, one can exploit the advantages of localized surface plasmon resonances (LSPR's), which provide large optical cross sections, high sensitivity to environmental changes, and large field enhancements<sup>20,21,22,23</sup>. This has led to a wealth of studies at the boundary between plasmonics and optical manipulation<sup>6,24,25,26,27</sup>. The strong light-matter interaction provided by LSPR has enabled us to design a platform where circularly polarized laser tweezers are capable of driving gold nanorods to spin at record rotation frequencies in water<sup>2</sup>. By tracking the Brownian motion of a rotating nanorod, detailed information about its environment and temperature can be obtained<sup>3,5</sup>. Simultaneous spectroscopic analysis provides an additional independent information channel for analysing local temperature and the morphological stability of the rotating nanorod<sup>1</sup>. A range of systems and configurations have been used for studying and applying rotary motion in optical tweezers, generating important insights within the field<sup>15,28,29,30,31,32</sup>. However, most of these studies have dealt with objects several micrometers in diameter while a single nanorod gives access to the nanometer size regime. Furthermore, when gold nanorods are used as the rotary nanomotor, torque is efficiently transferred mainly *via* scattering<sup>2,33</sup>. This decreases the risk of overheating the trapped particle<sup>3,34,35</sup>.

In the following method, we outline the steps required to build a system capable of efficient optical trapping and rotation of metal nanoparticles. The gold nanorods considered in these studies have high scattering cross sections, and the radiation pressure turns out to be stronger than the counteracting gradient force in the propagation direction. To still confine the particles in 3D, we utilize the force balance between Coulomb repulsion from a glass surface and the laser scattering force in the propagation direction. This 2D-trapping configuration greatly expands the range of trappable particles, as compared to standard 3D optical tweezers, and it can be easily combined with dark-field optical imaging and spectroscopy.

A trapped and rotating metal nanoparticle interacts with its environment, and detailed information about this interaction is contained in its motion and spectral properties. After describing how to construct the circularly polarized optical tweezers, we therefore also outline how to integrate instrumentation for probing rotational dynamics and for measuring Rayleigh scattering spectra in the experimental setup. The result is a versatile platform for studies of nanoscale rotation phenomena in physics, chemistry, and biology.

This protocol assumes that the researcher has access to suitable colloidal metal nanoparticles, preferably single crystalline gold nanorods. Gold nanorods can be purchased from specialized companies or synthesized in house using wet-chemistry methods. The nanorods used in our experiments were made by the seed-mediated growth method described in Ye *et al.* 2013<sup>36</sup>. It is advantageous if the morphology and optical properties of the nanoparticles are well characterized, for example using scanning electron microscopy (SEM) and optical extinction measurements. **Figure 1** displays data recorded from such measurements for representative nanorod types<sup>1</sup>.

An outline of the protocol is as follows: In the first section, we describe the construction of the optical tweezers based on circular polarization. In the second section, we describe how to extract information from the nanomotor by recording its rotational dynamics and scattering properties. The rotation frequency and the rotational Brownian motion of the trapped particle is measured using photon correlation spectroscopy by projecting backscattered laser light filtered through a linear polarizer on a fast single-pixel detector<sup>3</sup>. By fitting the data to a theoretical autocorrelation function, both the rotation frequency and the decay time of the rotational Brownian diffusion can be extracted<sup>2,3</sup>. The optical properties of the trapped and rotating nanoparticle are measured using dark field spectroscopy, which provides complementary information on the particle and its environment. In the third section, we describe the experimental procedure for the trapping and rotation of gold nanorods.

The protocol described up to this point is a straightforward path to a functioning circularly polarized optical tweezers system for nanoparticle rotation. However, sometimes issues arise that demand additional attention. In the fourth section, we outline a few of the common problems that we have encountered and how to address them. These include issues related to nanoparticle optical properties leading to poor trap stability (4.1), low rotation frequencies due to suboptimal circular polarization caused by beamsplitter birefringence (4.2), sticking of nanoparticles at the glass surface due to insufficient Coulomb repulsion (4.3), and deviation from the characteristic autocorrelation signal (4.4).

## Protocol

### 1. Circularly Polarized Optical Tweezers for Nanoparticle Rotation

- Construct the setup around a suitable inverted microscope and use a visible red-wavelength laser (660 nm). A schematic of the experimental setup is presented in **Figure 2**. Make sure to choose a laser with a stable output power up to 500 mW (producing a power at the sample plane of around 50 mW). Also ensure that the rest of the components perform well at the trapping laser wavelength.
- Use a dry objective with a numerical aperture (NA) of 0.95 and 40X magnification.
- Always wear safety goggles and maintain good laser security (especially if using non-visible lasers). Perform alignment on the minimum laser power. Encapsulate the whole laser path for both safety and to avoid thermal drift and dust in the light path.  
NOTE: Depending on the polarization state of the output from the laser, the optical tweezers could benefit from placing a linear polarizer as the initial optical component. If the polarization of the laser is already linear, this component can be omitted.
- Use a pair of positive lenses in a Keplerian telescope configuration (lenses at bottom of **Figure 2**) to expand the laser beam such that the beam diameter is slightly larger than the back aperture of the trapping objective.  
NOTE: This enables use of the entire NA of the objective and will produce a diffraction limited focus of the trap<sup>11</sup>, resulting in optimal trapping stiffness.
- Make sure that the trapping laser is properly collimated after the beam expander. This can be done by making sure the beam size is close to unchanged when propagating to the objective (or by using a shearing interferometer).
- Use two mirrors (M1 and M2 in **Figure 2**), mounted on kinematic mirror mounts (and if needed, a translation stage), to direct the laser beam into the microscope setup.  
Note 1: Keep enough space between laser mirrors and microscope to be able to add additional optical elements such as waveplates and beamsplitters.  
Note 2: Make sure that the laser is always filtered away from the ocular or any other accessible light exiting the microscope.
- Use a beamsplitter (50/50 partial transmission/reflection is used here, but a dichroic could also work well) inside the microscope to couple laser light into the objective, without losing imaging and measurement capability in the microscope setup.
- Include a camera (see **Figure 2**) in the setup for subsequent experimental observation and for data recording. If a system without an ocular is used, this is vital for any alignment.
- Focus the laser on a glass slide or a mirror. If the laser is aligned and enters the objective at a correct angle, the laser intensity pattern is radially symmetric when changing the focus above and below the focal point.
- Fine-tune the angles of the laser mirrors (M1 and M2 in **Figure 2**) to obtain optimal laser alignment (as described in 1.9).
- Circularly polarize the laser light.
  - On the light path to the objective, pass the laser through a quarter-wave plate (QWP;  $\lambda/4$  in **Figure 2**) oriented with its fast axis at 45° to the linear polarization of the laser light to convert the linearly polarized light into circularly polarized light at the sample plane.
  - Set up a 360°-rotatable linear polarizer and a power meter in front of the objective.
  - Check polarization by rotating the linear polarizer and noting the maximum and minimum power, corresponding to the major and minor axis or the polarization ellipse.  
NOTE: The ratio should be higher than 0.9 for optimal rotation performance. If this is not reached, see step 4.2 for a solution.
- Measure the laser power at the sample plane.
  - Use an optical power meter to probe the laser power at the sample plane. Take care to collect all the light passed through the objective for a correct gauging of trapping power.
  - Perform a linear sweep of output laser powers and record the corresponding powers at the sample plane for subsequent conversion to power density in the trap.

13. Set up a dark field (DF) system in Köhler illumination using an oil immersed DF condenser to enable visualization of particles and trapping events. This will allow for both imaging and spectroscopic measurements of the trapped nanoparticles.

## 2. Instrumentation for Measurements of Rotation, Rotational Brownian Dynamics, and Spectroscopic Properties

1. Photon correlation spectroscopy using a single-pixel detector.
  1. Insert a beamsplitter (30R/70T) into the optical path in order to extract backscattered light from the nanoparticle.
  2. Connect a fast single-pixel Si photodiode to a data acquisition card to enable recording of signals.  
NOTE: It is important to have a photodiode/DAQ that is capable of measuring the rotational frequencies expected (several tens of kHz).
  3. Focus light onto a collection fiber fixed in a *xy*-translation mount. Insert a linear polarizer before the collection fiber.
  4. For collection fiber alignment, couple visible light to the exit end of the fiber to illuminate the substrate. This allows visualization and analysis of the collection region of the fiber.
  5. Adjust the position of the fiber using the *xy*-translation mount, so that its collection region coincides with the position of the optical trap. Connect the exit end of the fiber to the Si-detector and fine tune the position of the fiber to maximize the collected back scattered signal.
2. Dark field spectroscopy setup.
  1. Bear in mind that care needs to be taken in choosing all optical components in the path between the sample and spectrometer, in order not to block light within the spectral range of interest.
  2. Take caution as direct scattered and/or reflected laser light might damage the spectrometer sensor. Block the laser light using appropriate filters and/or dichroic beamsplitters. Always perform alignment of the setup on the minimum laser power.
  3. Insert a beamsplitter/mirror in the optical path to redirect light to the spectrometer (in this protocol, a free-space coupled spectrometer is used). One of the microscopes output ports could also be used, if suitable.
  4. Use notch filters to remove the intense trapping laser light (filters of total OD12 at the laser wavelength were needed for sufficient blockage in our case), which in other case will obscure the spectral response of the nanoparticle of interest.
  5. Adjust the position of the optical tweezers by the guiding mirrors (M1 and M2 in **Figure 2**) so it coincides with the position of the spectrometer slit.  
Note 1: Changes in position of the optical trap will require realignment of the photon correlation measurement system (instructions 2.1.4-2.1.5).  
Note 2: At the new position of the optical tweezers, instructions 1.9-1.10 need to be repeated to reach a well aligned optical trap.

## 3. Experimental Procedure

1. Preparation of particles for experiments.
  1. Dilute the particles in DI-water. An appropriate concentration of nanorods should be in a range between 0.1-0.01 pM. Sonicate the diluted solution in an ultrasonic cleaner bath for 2 min to break apart possible aggregates and homogenize solution.
  2. Tune the concentration of nanorods in the dilution in order to avoid trapping of multiple particles. The longer the experiment that will be performed, the lower the concentration required to reduce the risk of trapping multiple particles or contaminations.
2. Preparation of sample cell.
  1. Wash a microscope slide and a cover glass (No. 1.5) in acetone and subsequently isopropanol under sonication for five minutes, respectively.  
NOTE: Make sure that the surface charge of the glass slide during experiment has the same polarity as the colloidal nanoparticles. Nanoparticles stabilized by the surfactant hexadecyltrimethylammonium bromide (CTAB) are positively charged.
  2. Place a 100  $\mu\text{m}$  spacer tape well on the glass slide.
  3. Disperse 2  $\mu\text{L}$  of the diluted nanoparticle solution on the microscope slide within the well and 2  $\mu\text{L}$  on the cover glass. Solution on both surfaces allows for a more controllable assembly of the sample cell.
  4. Connect the two parts of the sample cell together while avoiding forming any air bubbles inside the chamber.
  5. Place the cell on the microscope stage and place a drop of index-matched (immersion) oil on top of the sample and one drop on the condenser. Drops on each side avoid bubbles in the oil that scatters light and reduces the contrast of the DF illumination.
3. Performing an experiment.
  1. Locate a particle through observation in the DF imaging system. A single nanorod can usually be identified through observation of its Brownian motion (more erratic than aggregates) and color (corresponding to the strongest LSPR resonance).
  2. Start/unblock the trapping laser.
  3. Through a series of stage movement and focus corrections, push the chosen particle *via* radiation pressure in the laser's propagation direction towards the water-glass interface. At the interface, the *z*-movement is constrained by a balance between radiation pressure and Coulomb repulsion between CTAB molecules on the nanoparticle surface and the positively charged surface. The *xy*-fluctuations are confined by gradient forces in the optical tweezers.
  4. Through small focus corrections, maximize trapping stability or rotation speed, gauged from the autocorrelation data (as described below in instruction 3.4).
  5. At this point, record both rotational dynamics and spectroscopic properties of the trapped nanorod. See instructions 3.4 and 3.5 below on how to probe these. This can be done over extended periods of time, up to several hours if needed.
4. Rotational dynamics measurements.
  1. Make sure to have a collection region from the fiber that is large enough to always enclose the image of the particle during its translational motion.

2. Collect intensity oscillation signal with the Si photodetector at an appropriate probing frequency and collection time. Choose 65536 Hz and 1 s acquisition time to start with and adjust if needed.  
NOTE: Probing frequency should be at least two (and optimally ten) times larger than the rotation frequency multiplied by the degree of detectable rotational symmetry (N, see below). Collection time should be long enough to be able to obtain frequencies significantly lower than the rotation frequency.
3. After having collected a set of intensity fluctuation data from a rotating nanoparticle, calculate the autocorrelation of the intensity fluctuation. This is done by calculating the correlation of the signal with a time-delayed copy of itself for each delay time  $\tau$  (i.e.,  $C(\tau) = \{I(\tau) \cdot I(0)\}$ ).
4. Perform a fit to the theoretical autocorrelation function

$$C(\tau) = I_0^2 + \frac{I_1^2}{2} \exp\left(-\frac{\tau}{\tau_0}\right) \cos(2N\pi f_{\text{rot}}\tau)$$

where  $I_0$  is the average intensity,  $I_1$  is the amplitude of the intensity fluctuation and N is the degree of detectable rotational symmetry (for rod-like particles  $N=2$ )<sup>2,3</sup>.

5. From the fit, extract the rotation frequency  $f_{\text{rot}}$  and decay time of the autocorrelation signal  $\tau_0$  (related to rotational Brownian motion dynamics).
5. Spectroscopic measurements.
  1. Record a white light spectrum ( $I_{\text{white}}(\lambda)$ ) by collecting illumination light. This can be done by densely dispersing uniformly scattering polystyrene beads on a surface and collecting their scattering response.
  2. Record a background spectrum ( $I_{\text{bkg}}(\lambda)$ ) by collecting the stray light in the trapping spot when a particle is not trapped.  
Note 1: This should be done for each individual measurement, since background properties can vary significantly between different sample cells and even locations within a sample.  
Note 2: Recording background spectra should be done for the same laser power as used for optical trapping. This allows one to remove any possible auto-fluorescence from the glass slide, excited by the high laser intensities in the focus.
  3. Record a dark spectrum ( $I_{\text{dark}}(\lambda)$ ), when blocking all the light coming to the detector. Then, record a raw spectrum of a trapped nanoparticle ( $I_{\text{raw}}(\lambda)$ ).
  4. Access the actual nanoparticle scattering spectrum by calculating

$$I_{\text{scatt}}(\lambda) = \frac{I_{\text{raw}}(\lambda) - I_{\text{bkg}}(\lambda)}{I_{\text{white}}(\lambda) - I_{\text{dark}}(\lambda)}$$

5. To extract information about the LSPR peak positions, fit the DF scattering spectrum in energy scale with a bi-Lorentzian fitting function including a linear correction term for interband transitions in gold. The model function reads:

$$I(E) = I_B + kE + \frac{I_1\Gamma_1}{4(E-E_{0,1})^2 + \Gamma_1^2} + \frac{I_2\Gamma_2}{4(E-E_{0,2})^2 + \Gamma_2^2}$$

where  $E$  is the energy,  $I_B$  is a baseline intensity,  $k$  the slope of the linear correction,  $I_i$  are intensity maxima,  $\Gamma_i$  the full width at half maxima (FWHM) and  $E_{0,i}$  the peak positions of the two Lorentzian peaks.

## 4. Troubleshooting and solution to common problems

1. Problems related to gold nanorod properties.
  1. Poor trapping stability.
    1. Make sure that the main resonance (usually longitudinal resonance in case of nanorods) is on the blue wavelength side of the trapping laser wavelength. If not, the gradient force will become repulsive instead of attractive<sup>37</sup>.
    2. As a nanorod's size decreases, the motion from Brownian fluctuations increases, and at the same time the stabilizing force from Stokes drag decreases. Assure the nanorods are large enough for the  $xy$ -gradient force to overcome these destabilizing forces.
  2. Overlapping or broad spectral features.
    1. Rods need to have a large enough aspect ratio for LSPR peaks to be sufficiently separated to be individually resolved (see **Figure 1b**).  
NOTE: The laser wavelength puts an upper limit for the shape anisotropy, since the longitudinal LSPR redshifts for longer rods.
    2. The nanoparticles should preferably be small enough to not support higher order LSPR modes in the visible regime, since this complicates the analysis. Nanoparticle selection is a balance between this consideration and the trapping stability issue in instruction 4.1.1.2.
2. Inadequate circular polarization of trapping laser.
 

NOTE: To obtain the optimal performance of rotation of the trapped nanoparticle, the laser light reaching the specimen plane should be circularly polarized. Beamsplitters and other optical components can be polarization dependent, which might make it impossible to obtain perfect circular polarization using only a QWP.

  1. Insert a half-wave plate (HWP;  $\lambda/2$  in **Figure 2**) after the QWP in the path, to compensate for beamsplitter birefringence.
  2. Set up the linear polarizer and power meter configuration and perform an analysis of the laser's polarization state (as in instructions 1.11.2-1.11.3).
  3. For each position in increments of five degrees of the QWP, rotate the HWP through its entire angular range ( $90^\circ$ ) in steps of five degrees and measure the power ratio for each position. Strive to find the angles of QWP and HWP that maximize the ratio between maximum and minimum power.

NOTE: In our experience, the maximum ratio between the maximum and minimum powers was 0.75 without and 0.98 with the HWP correction.

3. Particles sticking to interface at laser power inadequate to confine particles in the *xy*-plane.
    1. Tune the concentration of stabilizing surfactant, through a particle washing procedure and subsequent re-dispersion of the nanorods in a controlled concentration of CTAB.
      1. Centrifuge the stock solution of nanoparticles until particles sediment (~5 min at 600g).
      2. Remove the suspension liquid.
      3. Re-disperse in water. This dilutes the CTAB content of the stock solution.
      4. Repeat steps 4.3.1.1. and 4.3.1.2. once more.
 

NOTE: Since CTAB acts as the colloid stabilizing agent, avoid excessive centrifugation time and speed in succeeding washing steps since the risk of aggregation increases as the CTAB is washed away.
    5. Most of the CTAB surfactants in the original colloidal solution is now removed and a new, well controlled, concentration of CTAB can be introduced to the colloid. From our experience, dispersing the stock solution in water with 20  $\mu\text{M}$  of CTAB and subsequent DI-water dilution to the experimental solution concentration results in a surface coverage that produces sufficient Coulomb repulsion.
    6. Possible fine tuning of the CTAB concentration might be needed to create appropriate particle/surface repulsion for the particular batch of nanoparticles used. Iterate the above procedure and slightly alter the CTAB concentration to find a proper one.
  2. Glass surface washing to negatively charge surface.
 

NOTE: This washing procedure produces a negatively charged surface that will be coated with free CTAB molecules in the experimental solution, making it positive and electrostatically repulsive for the particle during 2D trapping.

    1. Take a microscope slide and clean it in a mixture of water and 2 wt% of basic detergent heated to 80  $^{\circ}\text{C}$  for about 10 minutes until the surface is visibly hydrophilic.
 

NOTE: Avoid washing glass slides too long or harshly, since this can make the glass surface porous and produce a multitude of contamination particles.
4. Problems with photon autocorrelation spectroscopy.
  1. Low amplitude of the intensity oscillations or noisy signal.
    1. Insert a bandpass filter (BP filter in **Figure 2**) before the collection fiber, which passes the laser light and blocks dark-field illumination light.
 

NOTE: In principle, the measurement works when collecting all light as well. However, unpolarized white light DF illumination efficiently excites out of plane modes, and since a nanorod rotates about its short axis in a plane normal to the optical axis, this is the out of plane transverse LSPR. This mode does not carry any shape anisotropy during rotation and collecting light from it only reduces the signal to noise ratio of the measurement.
  2. Additional decay in autocorrelation function.
    1. Make sure the core size of the collection fiber is large enough to contain the image of the nanoparticle during all of its excursions due to translational Brownian motion.
    2. If a fiber with a too small core size is used, replace it with a larger one.
    3. Check alignment of the new fiber, as in instructions 2.1.4-2.1.5.

## Representative Results

The rotation and rotational Brownian motion of a gold nanorod that is properly trapped in the circularly polarized laser tweezers can be probed by recording light scattering intensity fluctuations (**Figure 3a**) using a single-pixel detector. An autocorrelation spectrum of this signal contains an oscillatory component, similar to the one shown in **Figure 3b**, which can be fit to a theoretical autocorrelation function. The fitting allows extraction of the rotation frequency and the autocorrelation decay time, which is related to the rotational Brownian fluctuations, of the nanorod.

As mentioned in the protocol (instruction 4.4.2), it is essential to use a sufficiently thick fiber core to collect the backscattered laser light for photon correlation spectroscopy. If this is not the case, an additional decay term related to particle translation in and out of the probe volume will be present in the correlation function, see **Figure 4**. Through careful analysis, this could provide more information about the system; however, it complicates the analysis of the rotational Brownian dynamics contained in the data.

To obtain correct DF scattering spectra from trapped nanoparticles, as described in section 3.5, the raw spectral data needs to be calibrated. This is done by recording the illumination lamp spectrum as well as a background spectrum (**Figure 5a**). When focusing intense laser light at a glass surface, such as the substrate against which the nanorods are trapped, some fluorescence might be generated (see the red spectral contribution in the background spectrum of **Figure 5a**). This fluorescence contamination can be reduced by using fused silica substrates. However, it is anyway highly recommended to record a background spectrum with empty optical tweezers at the correct laser power. When a scattering spectrum is recorded and all spectral components not related to the actual nanoparticle scattering have been compensated for, the spectrum can be fitted in energy scale with a bi-Lorentzian fitting function to extract information related to the LSPR peak positions (**Figure 5b**).

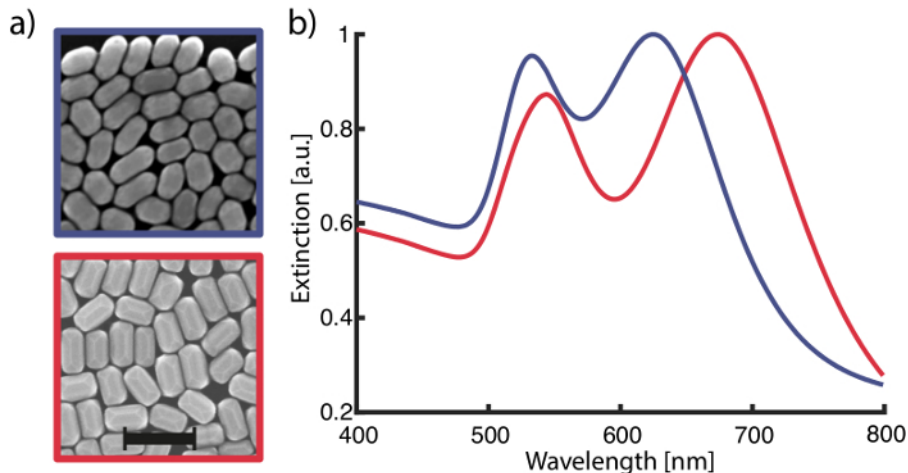


**Figure 1: SEM images and ensemble extinction spectra for two representative nanoparticle batches.** a) Scale bar is 200 nm. b) The blue/red bordered SEM images in a) correspond to the red/blue spectrum, respectively. The spectral peaks related to the transverse and longitudinal LSPRs are clearly distinguishable. [Please click here to view a larger version of this figure.](#)

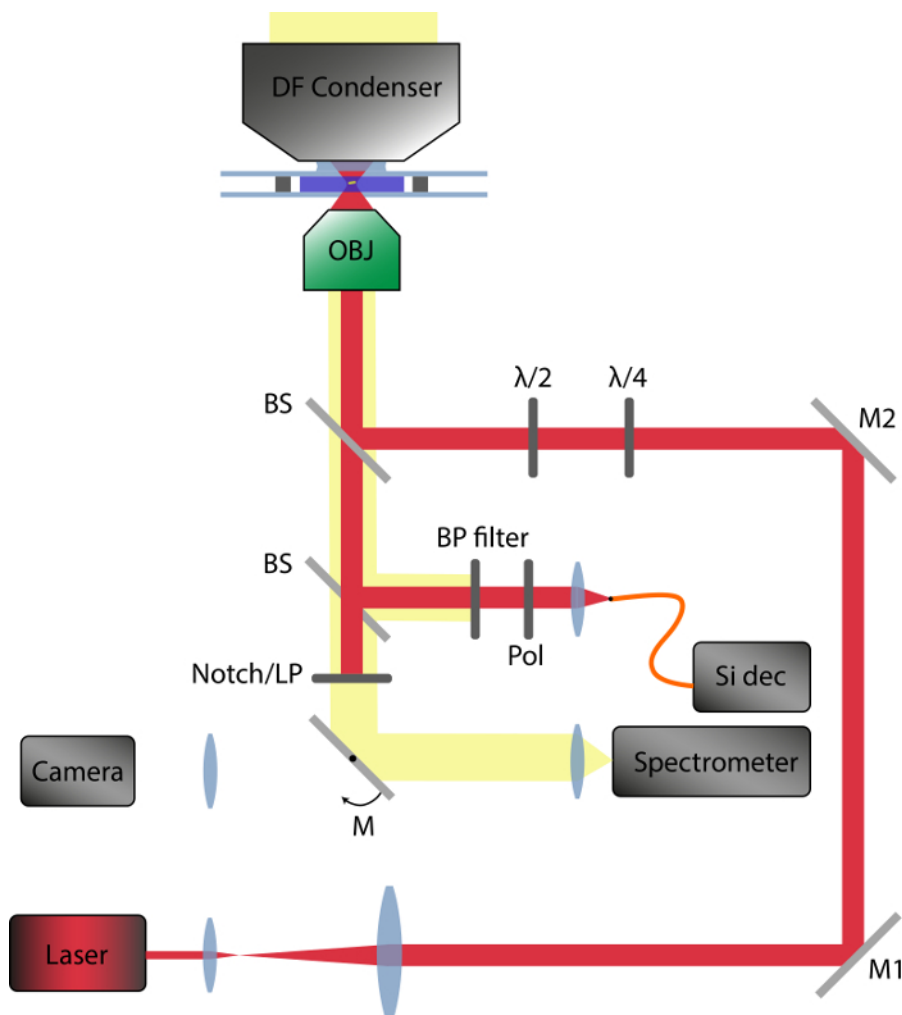


**Figure 2: Schematic illustration of optical tweezers setup for nanoparticle rotation measurements.** Laser light is collimated and expanded through a Keplerian telescope, and subsequently guided to the objective through the use of two movable mirrors (M1, M2) and a beamsplitter (BS). Two waveplates in the laser path optimize the circular polarization of the optical tweezers ( $\lambda/2$ ,  $\lambda/4$ ). Backscattered laser light can be collected after a linear polarizer for photon correlation spectroscopy and rotational dynamics measurements. After removing the laser light, scattered white light is guided to a spectrometer or a camera. [Please click here to view a larger version of this figure.](#)

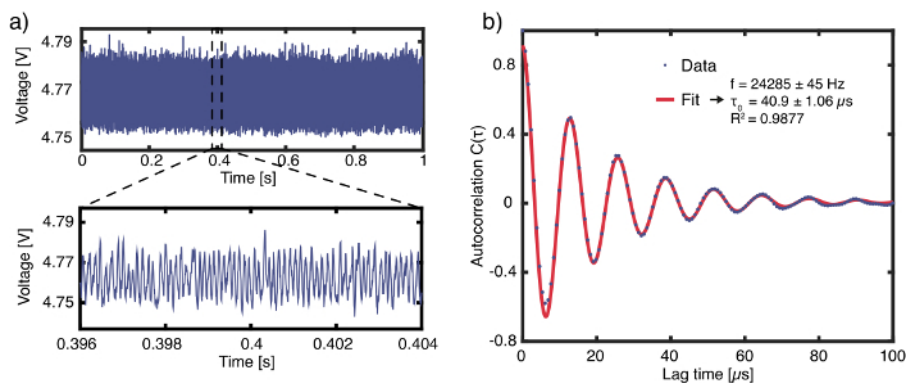


**Figure 3: Representative intensity and autocorrelation data with curve fit for a trapped and rotating nanorod.** **a)** Intensity fluctuations recorded by the single pixel detector after a linear polarizer for 1s, and a zoomed in plot of the fluctuations. **b)** Autocorrelated data of intensity fluctuation for a rotating gold nanorod (blue points), collected from backscattered laser light. The data shows an oscillation that decays after a few periods. The oscillation is related to the rotation frequency of the nanorod, whereas the decay is due to rotational Brownian motion. A fit to the theoretical autocorrelation function is performed (red line) to extract a rotation frequency of  $f = 24285 \pm 45$  Hz and a correlation decay time of  $\tau_0 = 40.9 \pm 1.06 \mu\text{s}$ . The  $f$  and  $\tau_0$  uncertainties represent 95% confidence intervals of the fit, which has a coefficient of determination ( $R^2$ ) of 0.9877. [Please click here to view a larger version of this figure.](#)

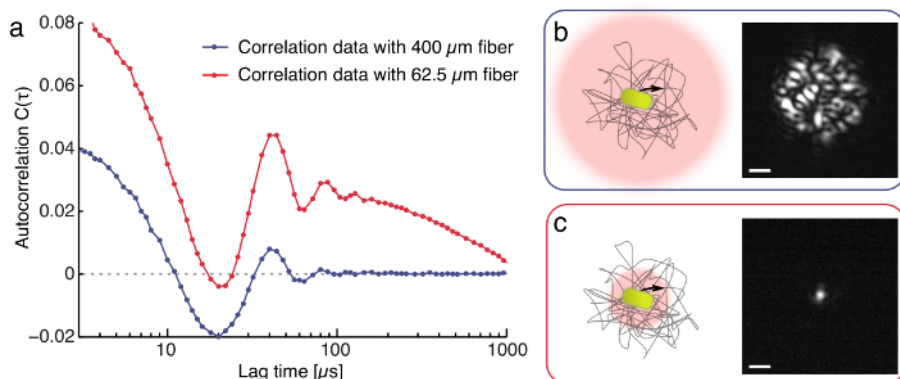


**Figure 4: Issue with a too small probe volume in photon correlation spectroscopy measurements.** **a)** Autocorrelation data for a rotating gold nanorod, collected using a thick ( $400 \mu\text{m}$ , blue data) and a thin ( $62.5 \mu\text{m}$ , red data) fiber. Collection using a thick fiber ensures that the nanorod is always confined within the probe volume and that the autocorrelation function measures rotational dynamics only. An additional decay term due to translational Brownian motion is present when the probe volume is insufficient. In **b)** and **c)**, schematic illustrations of the effect and images of the back-illuminated collection region are shown. Scale bars are  $2 \mu\text{m}$ . [Please click here to view a larger version of this figure.](#)

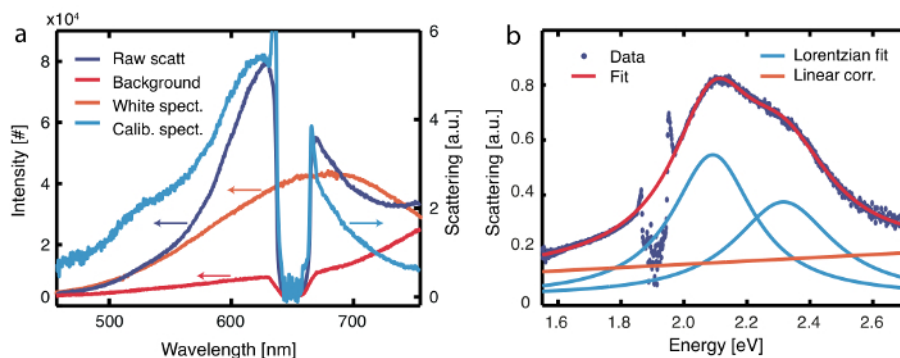


**Figure 5: Exemplary dark field scattering spectra recorded for a gold nanorod optically trapped by 660 nm laser light.** The spectral region 630–670 nm (1.85–1.97 eV) is distorted due to notch filters needed to block the trapping laser light. **a)** Raw scattering spectra (dark blue) displaying features that are not inherent to the scattering of the particle and should be calibrated for. These include the background spectrum (red), which contains autofluorescence excited by the highly focused laser light, and the white light excitation spectrum (orange, recorded without notch filter). After calibration, the corrected scattering spectrum (light blue) shows two distinct LSPR peaks as expected. The arrows indicate the scale for each spectrum. **b)** Scattering spectrum for a trapped nanorod (blue points) together with a fit to the bi-Lorentzian model function (red) with its components (light blue and orange). The distorted spectral region is disregarded in the fitting of the data and the fit has an  $R^2$  of 0.9975. [Please click here to view a larger version of this figure.](#)

## Discussion

The optical trapping setup described in this protocol is built around a commercial inverted microscope and uses red laser light. However, the techniques outlined are versatile and can be used to construct circularly polarized optical tweezers around most commercial or home-built microscopes, both upright and inverted, with only slight alterations. The trapping laser wavelength can be chosen within a wide visible-NIR spectrum, as long as the rest of the optical components and detectors are functional at this specific wavelength. Nevertheless, when choosing a laser wavelength, the size and spectral vicinity to resonances of the particles to be manipulated should be considered because this will affect the optical trapping forces and rotation performance<sup>2,5</sup>, the magnitude of photothermal effects<sup>1</sup>, and the trapping stability<sup>26</sup>. We have previously successfully worked with circularly polarized laser tweezers using laser wavelengths of 660, 785, 830, and 1064 nm.

One of the most important components of the optical trapping setup is the microscope objective. The objective in this protocol is a dry objective with NA = 0.95. The use of a dry objective is experimentally a simpler realization of the setup; however, it does lead to optical aberrations due to refraction in the sample cell interfaces. In the present case, the result is a slightly enlarged focus spot (~1.2  $\mu\text{m}$ ) compared to the diffraction limit (~0.4  $\mu\text{m}$ ), but this does not significantly change the general or rotary performance of the platform. In principal, a wide range of microscope objectives can be used, provided they have good transmission at the trapping wavelength, good polarization maintenance and long enough working distance to perform trapping through a microscope cover slip and layer of water. In case of 2D trapping, the NA can be relatively low, which makes the entire experiment simpler and provides cleaner circular polarization in the focus. However, higher laser powers might be required than in case of a high NA objective. In our experience, the best performance for trapping, rotation and dark-field spectroscopy is obtained with objectives with NA 0.7-0.95, but it is possible to use lower as well as higher NA objectives.

To obtain good photon correlation measurements of rotary motion, a fast single-pixel detector is needed. Choose a detector with a bandwidth at least two, preferably ten, times higher than the expected rotation frequency multiplied by the shape degeneracy factor and high sensitivity at the trapping wavelength used. Amplified Si photodetectors, single photon counting APDs, and PMTs have been used with success in different setups in our laboratories. Additional information, for example on trap stiffness, can be obtained by measuring and analyzing particle translational displacement using well-established techniques such as power spectral analysis<sup>5</sup>. A number of previous publications describe different variants of this technique<sup>38,39</sup>. DF spectroscopy can be performed using a wide range free-space or fiber coupled spectrometers and the choice should be based on the spectral range and wavelength and temporal resolution needed for the planned study.

When performing a trapping experiment, additional particles may accidentally enter the trap. This can be detected by monitoring the rotation frequency, which will fluctuate strongly due to the disturbance. Visual inspection by DF microscopy can be used to verify the presence of an additional particle, in which case the stage can be moved to avoid further disturbance or the experiment needs to be restarted.

The system described above is a simple and efficient way to realize 2D confinement and rotation of metallic nanoparticles. However, for some applications, the extra degree of freedom for manipulation that comes with 3D trapping is important, and the current configuration is therefore a limitation. However, 3D confinement and rotation might be achievable by utilizing counter propagating laser tweezers or more exotic trapping configurations.

Although the particle and system parameters discussed here can be optimized to reduce photothermal heating to below ~15 K<sup>4</sup>, the temperature increase associated with plasmonic excitation of metal nanoparticles can be problematic in certain applications. A possible route towards further heat reduction is to use high-index dielectric nanoparticles instead of plasmonic particles. Such particles support strong Mie-type scattering resonances but at the same time exhibit low intrinsic absorption coefficients. We have recently been able to manufacture colloidal resonant Si nanoparticles that might prove useful in this respect<sup>40,41</sup>.

## Disclosures

The authors have nothing to disclose.

## Acknowledgements

This work was supported by the Knut and Alice Wallenberg Foundation, the Swedish Research Council and the Chalmers Area of Advance Nanoscience and Nanotechnology.

## References

1. Andr n, D. *et al.* Probing photothermal effects on optically trapped gold nanorods by simultaneous plasmon spectroscopy and brownian dynamics analysis. *ACS Nano*. **11** (10), 10053-10061 (2017).
2. Shao, L., Yang, Z.-J., Andr n, D., Johansson, P., & K ll, M. Gold nanorod rotary motors driven by resonant light scattering. *ACS Nano*. **9** (12), 12542-12551 (2015).
3. Lehmuskero, A., Ogier, R., Gschneidner, T., Johansson, P., & K ll, M. Ultrafast spinning of gold nanoparticles in water using circularly polarized light. *Nano Letters*. **13** (7), 3129-3134 (2013).
4.  ipova, H., Shao, L., Odebo Lank, N., Andr n, D., & K ll, M. Photothermal DNA release from laser-tweezed individual gold nanomotors driven by photon angular momentum. *ACS Photonics*. Accepted (2018).
5. Hajizadeh, F. *et al.* Brownian fluctuations of an optically rotated nanorod. *Optica*. **4** (7), 746-751 (2017).
6. Tong, L., Miljkovic, V. D., & K ll, M. Alignment, rotation, and spinning of single plasmonic nanoparticles and nanowires using polarization dependent optical forces. *Nano Letters*. **10** (1), 268-273 (2009).

7. Lehmuskero, A., Li, Y., Johansson, P., & Käll, M. Plasmonic particles set into fast orbital motion by an optical vortex beam. *Optics Express*. **22** (4), 4349-4356 (2014).
8. Lehmuskero, A., Johansson, P., Rubinsztein-Dunlop, H., Tong, L., & Käll, M. Laser trapping of colloidal metal nanoparticles. *ACS Nano*. **9** (4), 3453-3469 (2015).
9. Shao, L., & Käll, M. Light-driven rotation of plasmonic nanomotors. *Advanced Functional Materials*. In Press (2018).
10. Ashkin, A., Dziedzic, J. M., Bjorkholm, J., & Chu, S. Observation of a single-beam gradient force optical trap for dielectric particles. *Optics letters*. **11** (5), 288-290 (1986).
11. Neuman, K. C., & Block, S. M. Optical trapping. *Review of scientific instruments*. **75** (9), 2787-2809 (2004).
12. Chu, S., Hollberg, L., Bjorkholm, J. E., Cable, A., & Ashkin, A. Three-dimensional viscous confinement and cooling of atoms by resonance radiation pressure. *Physical Review Letters*. **55** (1), 48 (1985).
13. Svoboda, K., & Block, S. M. Optical trapping of metallic Rayleigh particles. *Optics Letters*. **19** (13), 930-932 (1994).
14. Wang, M. D., Yin, H., Landick, R., Gelles, J., & Block, S. M. Stretching DNA with optical tweezers. *Biophysical journal*. **72** (3), 1335-1346 (1997).
15. Frieze, M. E. J., Nieminen, T. A., Heckenberg, N. R., & Rubinsztein-Dunlop, H. Optical alignment and spinning of laser-trapped microscopic particles. *Nature*. **394** (6691), 348-350 (1998).
16. Gao, W., & Wang, J. Synthetic micro/nanomotors in drug delivery. *Nanoscale*. **6** (18), 10486-10494 (2014).
17. Li, M., Lohmüller, T., & Feldmann, J. Optical injection of gold nanoparticles into living cells. *Nano Letters*. **15** (1), 770-775 (2014).
18. Nelson, B. J., Kaliakatsos, I. K., & Abbott, J. J. Microrobots for minimally invasive medicine. *Annual review of biomedical engineering*. **12** 55-85 (2010).
19. Balk, A. L. *et al.* Kilohertz rotation of nanorods propelled by ultrasound, traced by microvortex advection of nanoparticles. *ACS Nano*. **8** (8), 8300-8309 (2014).
20. Chen, H., Shao, L., Li, Q., & Wang, J. Gold nanorods and their plasmonic properties. *Chemical Society Reviews*. **42** (7), 2679-2724 (2013).
21. Maier, S. A. *Plasmonics: fundamentals and applications*. Springer Science & Business Media (2007).
22. Xu, H., Bjerneld, E. J., Käll, M., & Börjesson, L. Spectroscopy of single hemoglobin molecules by surface enhanced Raman scattering. *Physical Review Letters*. **83** (21), 4357 (1999).
23. Chen, H., Kou, X., Yang, Z., Ni, W., & Wang, J. Shape- and size-dependent refractive index sensitivity of gold nanoparticles. *Langmuir*. **24** (10), 5233-5237 (2008).
24. Ruijgrok, P. V., Verhart, N. R., Zijlstra, P., Tchebotareva, A. L., & Orrit, M. Brownian fluctuations and heating of an optically aligned gold nanorod. *Physical Review Letters*. **107** (3), 037401 (2011).
25. Pelton, M. *et al.* Optical trapping and alignment of single gold nanorods by using plasmon resonances. *Optics Letters*. **31** (13), 2075-2077 (2006).
26. Hansen, P. M., Bhatia, V. K., Harrit, N., & Oddershede, L. Expanding the optical trapping range of gold nanoparticles. *Nano Letters*. **5** (10), 1937-1942 (2005).
27. Ni, W., Ba, H., Lutich, A. A., Jäckel, F., & Feldmann, J. Enhancing Single-Nanoparticle Surface-Chemistry by Plasmonic Overheating in an Optical Trap. *Nano Letters*. **12** (9), 4647-4650 (2012).
28. Liu, M., Zentgraf, T., Liu, Y., Bartal, G., & Zhang, X. Light-driven nanoscale plasmonic motors. *Nature nanotechnology*. **5** (8), 570-573 (2010).
29. Neale, S. L., MacDonald, M. P., Dholakia, K., & Krauss, T. F. All-optical control of microfluidic components using form birefringence. *Nature Materials*. **4** (7), 530-533 (2005).
30. Jones, P. *et al.* Rotation detection in light-driven nanorotors. *ACS Nano*. **3** (10), 3077-3084 (2009).
31. Bonin, K. D., Kourmanov, B., & Walker, T. G. Light torque nanocontrol, nanomotors and nanorockers. *Optics Express*. **10** (19), 984-989 (2002).
32. Arita, Y. *et al.* Rotational dynamics and heating of trapped nanovaterite particles. *ACS Nano*. **10** (12), 11505-11510 (2016).
33. Lee, Y. E., Fung, K. H., Jin, D., & Fang, N. X. Optical torque from enhanced scattering by multipolar plasmonic resonance. *Nanophotonics*. **3** (6), 343-350 (2014).
34. Kyrsting, A., Bendix, P. M., Stamou, D. G., & Oddershede, L. B. Heat profiling of three-dimensionally optically trapped gold nanoparticles using vesicle cargo release. *Nano Letters*. **11** (2), 888-892 (2010).
35. Andres-Arroyo, A., Wang, F., Toe, W. J., & Reece, P. Intrinsic heating in optically trapped Au nanoparticles measured by dark-field spectroscopy. *Biomedical Optics Express*. **6** (9), 3646-3654 (2015).
36. Ye, X., Zheng, C., Chen, J., Gao, Y., & Murray, C. B. Using binary surfactant mixtures to simultaneously improve the dimensional tunability and monodispersity in the seeded growth of gold nanorods. *Nano Letters*. **13** (2), 765-771 (2013).
37. Arias-González, J. R., & Nieto-Vesperinas, M. Optical forces on small particles: attractive and repulsive nature and plasmon-resonance conditions. *JOSA A*. **20** (7), 1201-1209 (2003).
38. Berg-Sörensen, K., & Flyvbjerg, H. Power spectrum analysis for optical tweezers. *Review of Scientific Instruments*. **75** (3), 594-612 (2004).
39. Gittes, F., & Schmidt, C. F. Interference model for back-focal-plane displacement detection in optical tweezers. *Optics Letters*. **23** (1), 7-9 (1998).
40. Verre, R. *et al.* Metasurfaces and colloidal suspensions composed of 3D chiral Si nanoresonators. *Advanced Materials*. **29** (29), (2017).
41. Verre, R., Odebo Länk, N., Andrén, D., Šípová, H., & Käll, M. Large-scale fabrication of shaped high index dielectric nanoparticles on a substrate and in solution. *Advanced Optical Materials*. In Press (2018).